J Therm Anal Calorim (2017) 128:1661–1669
DOI 10.1007/s10973-016-6022-5

Thermal decomposition of long-chain fatty acids and its derivative in the presence of montmorillonite

A thermogravimetric (TG/DTG) investigation

Hongling Bu[1,2] · Peng Yuan[1] · Hongmei Liu[1] · Dong Liu[1] · Xiang Zhou[1,2]

Received: 15 March 2016 / Accepted: 27 November 2016 / Published online: 22 December 2016

Abstract In sedimentary environments or clay-rich rocks, clay minerals are usually combined with organic matter; however, little research has focused on the effects of combinations of organic matter and clay minerals on the thermal degradation of organics and on subsequent hydrocarbon generation. In this study, the long-chain fatty acid octadecanoic acid (OA) and its derivative octadecy trimethyl ammonium bromide (OTAB) were selected as model organics. The organics were prepared for clay–organic associations with Na-based montmorillonite (Mt(Na)). The thermal decomposition behaviors of these associations were studied via thermogravimetric (TG/DTG) analysis. In the presence of Mt(Na), OA decomposed at 275.2 °C, decomposing sooner than pure OA. The thermal decomposition behavior of OTAB is nearly consistent with that of pure OTAB, but for interlayer OTAB, the decomposition temperature increased to higher than 300 °C. The results indicate that Mt(Na) plays a dual role in the thermal decomposition of fatty acid. Mt(Na) may accelerate the thermal decomposition of OA, and inherent solid acidity levels may be the key factor. In addition, the interlayer structure of Mt(Na) can increase the thermal stability of OA and OTAB. The above results further demonstrate that the thermal decomposition behavior of a given organic material may also depend on its structure and composition. In the presence of Mt(Na), organics with amino and amine structures are more stable than those with carboxyl groups.

Keywords Montmorillonite · OA · OTAB · TG · Thermal decomposition · Clay–organic complex

✉ Peng Yuan
yuanpeng@gig.ac.cn

[1] CAS Key Laboratory of Mineralogy and Metallogeny/Guangdong Provincial Key Laboratory of Mineral Physics and Materials, Guangzhou Institute of Geochemistry, Chinese Academy of Sciences (CAS), Guangzhou 510640, Wushan, China

[2] University of Chinese Academy of Sciences, Beijing 100049, China

Introduction

Clay minerals of the smectite group (e.g., montmorillonite (Mt)) have received particular attention owing to their known catalytic activities and to their ubiquity in low-maturity source rocks. The influence of Mt on catalyzing organic reactions has been studied by several researchers [1–8], and the catalytic effects of smectite have been confirmed. An important motivation behind these studies lies in the fact that organic matter always combines with clay minerals in source rocks, which are difficult to separate using physical methods [9, 10]. For this reason, several researchers have developed mixtures of clay minerals and organics by simply grinding clays with organics to simulate the natural combination of clay minerals and organic matter and to examine hydrocarbon generation mechanisms in the presence of clay minerals.

Organic matter in interlayer spaces of clay minerals constitutes one of the most important forms of combination between clay minerals and organic matter. Related evidence has been previously reported. The intercalation of organics into the interlayer space of Mt occurs through cationic exchange reactions whereby organic guests replace the original hydrated cations. This interlayer clay–organic association has been studied in soils by numerous researchers [11, 12]. From the results of these investigations, clay–organic compounds in sedimentary rocks have

gradually been revealed [7, 13, 14]. Lu et al. [13] detected approximately 25–50% of all interlayer organics via a supercritical fluid extraction (SFE) method in reference to swelling clay minerals of source rocks. In a recent study, Yuan et al. [15] studied the role of the interlayer space of Mt in hydrocarbon generation. An interlayer complex of Mt and 12-aminolauric acid (ALA) was prepared and used for high temperature and pressure pyrolysis experiments conducted in a flexible gold capsule. The authors found C_{1-5} hydrocarbons released from the interlayer complex pyrolysis and from the mixed complex that were approximately 43 and 5 times greater than amounts released from pure ALA, respectively. This finding implies that organics found in the interlayer space of Mt may present quite different thermal degradation behaviors from organics mixed with Mt. However, because the compositions of natural organic matter are highly complex, more related studies are needed to achieve a more comprehensive understanding of the role that clay minerals play in the thermal degradation of organics and in hydrocarbon generation. Unfortunately, studies focused on this topic have been rarely conducted until recently.

In particular, as an important form of clay–organic association, organic matter in the interlayer space of swelling clays has been proposed and confirmed by previous studies [16–18], and interlayer organics in source rocks have also been found [13, 14]. This suggests that the effect of the interlayer space within clay minerals on the evolution of natural organic matter is worthy of further investigation. Consequently, to clearly investigate interlayer organic–inorganic reactions through pyrolysis experiments, it is necessary to use high-purity and structurally simple synthetic organics as a model component for simulating clay–organic complexes [15, 19–21].

Long-chain fatty acid forms one of the main components of soluble organics, which are typically found in less mature oil source rocks. In this study, one type of long-chain fatty acid, octadecanoic acid ($CH_3(CH_2)_{16}COOH$ (abbreviated as OA), was used as a model organic material. OA was chosen as it is likely the most abundant carboxylic acid found in nature, and it contains carboxyl groups and alkyl chains with eighteen carbon atoms. During petroleum generation, fatty acid decarboxylation and subsequent cracking are assumed to serve as key processes [1, 2]. Therefore, OA is suited for use as a model organic material. Furthermore, a derivative of OA, octadecy trimethyl ammonium bromide ($CH_3(CH_2)_{17}N$ $(CH_3)_3Br$ (abbreviated as OTAB), is also used for purposes of comparison, as OA cannot be intercalated into the interlayer space of Mt under the applied conditions. OTAB was selected and prepared in an interlayer complex with Mt, and it has the same carbon chain as OA. Most importantly, it is a type of quaternary ammonium salt that can be intercalated into the interlayer space of Mt via cation exchange. The effects of Mt on long fatty acid thermal behavior were studied using the TG/DTG technique together with X-ray diffraction (XRD) and Fourier transform infrared (FTIR) analyses to further elucidate the interlayer configuration of intercalated organics in Mt. The comparative study results obtained from this study help to better elucidate the thermal degradation of this fatty acid.

Materials and methods

The Mt sample was obtained from an area in Inner Mongolia, China. A raw Ca-montmorillonite (Mt(Ca)) sample was purified by repeated sedimentation to remove impurities, and a <2 μm fraction was collected and used for our experiments. The purified samples were prepared by dispersing Mt in distilled water and were treated with 0.5 M sodium chloride solution under vigorous stirring at 80 °C for 24 h. The resultant solid was separated by centrifugation, and the product was again treated with sodium chloride solution; this process was repeated three times. The product was repeatedly rinsed with distilled water (until no chloridion ion was detected) and, then, freeze-dried for 48 h before being ground to a powder. The final sample was denoted as Mt(Na). OA and OTAB were purchased from Sigma–Aldrich (95%) and were used without further purification.

The simply mixed Mt(Na)-OA and Mt(Na)-OTAB complexes were prepared via the following method: 5 g of Mt(Na) sample and 1.25 g (20.0 mass%) of OA or OTAB were mixed and ground via ball milling for 20 min using a Pulverisette-6 Planetary Mill. The products are denoted as OA-Mt(Na) and OTAB-Mt(Na), respectively. The interlayer Mt(Na)-OTAB complex was prepared using the following procedure. 4.34 g of OTAB (equivalent to 1.0 times the CEC of Mt(Na)) was added to distilled water and stirred for 30 min at 60 °C. Then, Mt(Na) was added, and the mass ratio of water/clay reached 20:1. The solution was stored at 60 °C with water bath stirring for 12 h. Solids in the mixture were filtered and repeatedly washed with distilled water to remove excess OTAB ions and were then dried and ground to a powder. The product was labeled as $OTAB_{inter}$-Mt(Na), i.e., the clay–organic interlayer complex with Mt(Na) and OTAB.

X-ray diffraction (XRD) and Fourier transform infrared (FTIR) spectra were used in the study. A powdered XRD analysis was performed using a Bruker D8 Advance diffractometer with a Ni filter and Cu Kα radiation features (40 kV and 40 mA). The samples were collected from 1° to 30° at a scanning rate of 1°(2θ) min^{-1}. The FTIR spectra of the samples in the pressed KBr pellets were recorded using a Bruker Vertex-70 FTIR spectrometer. The spectra were

collected over a range of 400–4000 cm^{-1} with 64 scans at a resolution of 4 cm^{-1}.

A thermogravimetric (TG/DTG) analysis of the samples was performed using a Netzsch 449 C instrument. Approximately 5–10 mg of fine powder samples were heated from 30 to 1000 °C at a heating rate of 10 °C min^{-1} under a high-purity N_2 atmosphere (60 cm^3 min^{-1}).

A chemical element analysis of these interlayer complexes was conducted using an Elementar Vario EL III Universal CHNOS elemental analyzer. Slightly less than 10 mg of fine powder samples was prepared for this measurement.

The determination of cation exchange capacity (CEC) of clay was measured using cobalt hexamine chloride cation ($[Co(NH_3)_6]^{3+}$) exchange method by spectrophotometry. The cobalt hexamine chloride was purchased from Aldrich (98%) and used without further purification. Three parallel tests were conducted for the accuracy. 1-g dry weight Mt(Na) was placed in 50-mL polypropylene tubes and 20 mL of 0.025 mol/L cobalt hexamine chloride solution were added. After continuous shaking for 24 h on a rotating device, tubes were centrifuged at 7000 rpm for 10 min. The CEC value was evaluated by comparing the content of the cobalt cations (Co^{3+}) in the solution before and after the exchange of Mt(Na) with $[Co(NH_3)_6]^{3+}$, using the following equation.

$$\text{CEC value (mmol/100 g)} = 3 \times C \times V/M \times 100$$

where C (mmol L^{-1}) is the Co^{3+} concentration obtained by using a UV–Vis spectroscopy at wavelength of 472 nm; V (L) is the solution volume; and M (g) is the mass of Mt(Na). According to the results, the CEC of Mt(Na) is 110.5 mmol/100 g.

Results and discussion

Characterization of Mt(Na), the Mt(Na)-OA complex and the Mt(Na)-OTAB complex

The XRD patterns of Mt(Na), OA-Mt(Na), OTAB, OTAB-Mt(Na) and $OTAB_{inter}$-Mt(Na) are shown in Fig. 1. The basal spacing of Mt(Na) is 1.26 nm (Fig. 1a). For the Mt(Na)-OA complex, no change was observed in the (001) reflection relative to Mt(Na) (Fig. 1b), denoting that intercalation did not occur during the sample preparation phase. The same result is also observed for the OTAB-Mt(Na) sample (Fig. 1c). However, the basal spacing of $OTAB_{inter}$-Mt(Na) is 2.36 nm (Fig. 1d), denoting a successful intercalation of OTAB into the interlayer space of the Mt(Na). These results are consistent with previous work on alkylammonium intercalation [22–24]. The (002) diffractions with d-spacing are approximately 1.15 nm.

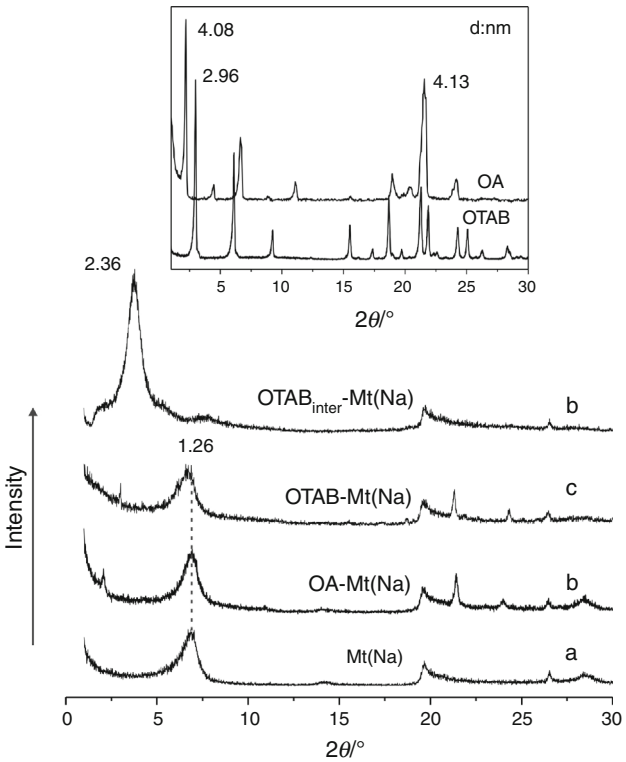

Fig. 1 XRD patterns of Mt(Na), OA, OTAB, Mt(Na)-OA and Mt(Na)-OTAB complexes

This suggests that the intercalation of OTAB occurs without destroying the layered structure of Mt(Na). The content of intercalated OTAB in $OTAB_{inter}$-Mt(Na) is 30.3 wt% as determined based on percentages of N (mass%) derived from the elemental analysis. The intercalated amount of OTAB in $OTAB_{inter}$-Mt(Na) is 77.0 mmol/100 g, which is lower than the CEC value (110.5 mmol/100 g) of Mt(Na). This result indicates that a small quantity of Na^+ may remain in the interlayer space of $OTAB_{inter}$-Mt(Na).

The FTIR spectra of the Mt(Na), OA, OTAB, Mt(Na)-OA and Mt(Na)-OTAB complexes are shown in Fig. 2. Main vibrations were assigned (Table 1) based on previous reports [23, 25, 26]. The FTIR spectrum of OA-Mt(Na) is a combination of characteristic bands of Mt(Na) and pure OA (Fig. 2a, b). The same phenomenon is found in OTAB-Mt(Na) (Fig. 2c). The results indicate that the raw materials are not changed by simple mechanical grinding, which is consistent with the XRD data.

However, several differences can be observed between the Mt(Na) and $OTAB_{inter}$-Mt(Na) spectra (Fig. 2d, e). As demonstrated by the FTIR spectra of $OTAB_{inter}$-Mt(Na), vibrations of the sorbed water of Mt(Na) at 1642 cm^{-1} are less intense than those of $OTAB_{inter}$-Mt(Na), implying that H_2O content levels are reduced with the replacement of hydrated sodium cations by OTAB [27]. Additionally, the

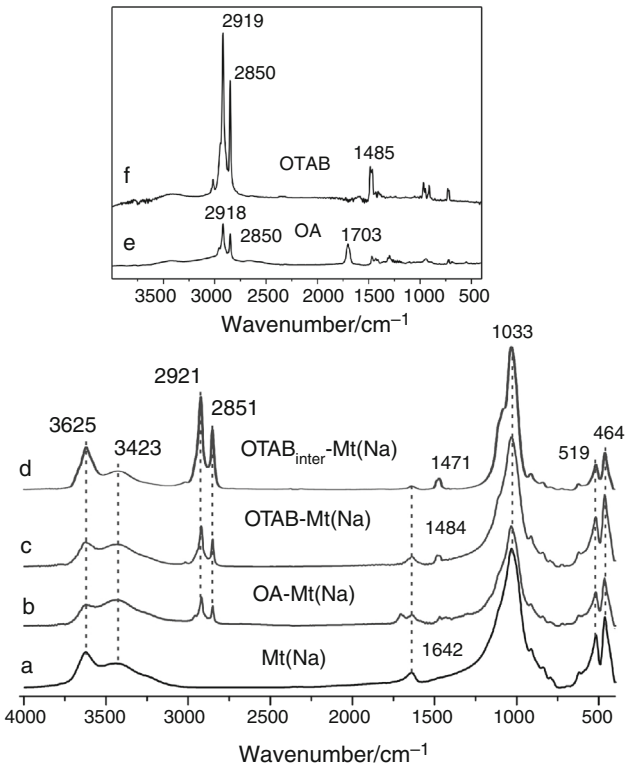

Fig. 2 FTIR spectra of Mt(Na), Mt(Na)-OA and Mt(Na)-OTAB complexes

Table 1 Band assignments of the FTIR spectra of samples

Wave number/ cm^{-1}	Bands
3625	O–H stretching of the structural hydroxyl group of Mt
3441/3423	O–H stretching of adsorbed water of Mt
2921	CH_2 antisymmetric stretching
2851	CH_2 symmetric stretching
1703	C=O stretching of OA
1642	O–H deformation of the water of Mt
~1484	CH_3 C–H antisymmetric bending in N^+-CH_3
1471	CH_2 deformation
1033	Si–O–Si stretching of Mt
519	Si–O–Al deformation of Mt
464	Si–O–Si bending of Mt

broad band at approximately 3441 (for Mt(Na)) cm^{-1} shifts to 3423 cm^{-1} through the O–H stretching of adsorbed water in Mt(Na). In addition, as shown in Fig. 2, the band at 1484 cm^{-1} and 1471 cm^{-1} is occurred in the spectrum of $OTAB_{inter}$-Mt(Na). The former is attributed to the antisymmetric bending mode of the head [$(CH_3)_3N^+$] methyl group, the latter is due to the CH_2 deformation mode. It means the OTAB has intercalated into the Mt(Na). The above phenomena indicate that hydrated sodium cations were replaced by the OTAB. However, a small quantity of Na^+ may remain in the interlayer space. This is also demonstrated by the element analysis results.

Thermal decomposition behaviors of pure organic matter and complexes

The TG and DTG curves of pure OA and OTAB are plotted in Fig. 3a, b. There is one peak on the DTG curve of OA, with a main thermal decomposition temperature of 323.7 °C and a mass loss of more than 90% (Table 2). During the thermal decomposition of OA, decarboxylation was likely the main reaction [28]. Unlike the pattern of OA, there are two peaks on the DTG curves of OTAB with an onset temperature of 266.2 °C and a small peak at 367.9 °C. This indicates that the thermal decomposition of OTAB mainly occurred at temperatures of 200–400 °C and that the greatest mass loss was approximately 90%. The first peak is attributed to the decomposition of OTAB, which represents the main thermal decomposition occurring at 266.2 °C. The small peak at 367.9 °C should be attributed to the thermal degradation of the carbonaceous residual organics.

For Mt(Na), no substantial differences from the results of other researchers were found. The thermal decomposition of Mt(Na) can be divided into two phases: (1) adjustment from room temperature to 200 °C due to dehydration (adsorption water and interlayer water) with a DTG peak at 104.8 °C; (2) followed by structural water (bonded hydroxyl that undergoes dehydroxylation) region development at 640.3 °C [29–31] (Fig. 3c; Table 2).

Figure 4 shows the TG and DTG curves of the Mt(Na)-OA complex. In the presence of Mt(Na), it is of interest to determine the thermal decomposition characteristics of OA, which differ from those of unaltered OA and which are nearly a combination of pure OA and Mt(Na) (Figs. 3, 4). The change in mass occurs over three stages: less than 200 °C, 200–500 °C, and higher than 500 °C. In the first stage, a thermal decomposition peak occurs at 99.7 °C in the DTG curve and a mass loss of up to 6.9% occurs (Table 2). This amount of mass loss is attributed to dehydration (adsorption water and interlayer water) in Mt(Na) as determined through a gas chromatograph (GC) analysis with TG instrumentation [23, 31]. In the second phase, the thermal decomposition peak occurs at a temperature of 275.2 °C with a percentage of mass loss corresponding to 19.9% (Table 2; Fig. 4). This mass loss is attributed to the thermal degradation of OA. A few small DTG peaks may be attributed to a small amount of OA that spontaneously decomposed and that remained unaffected by Mt(Na). Of course, the thermal decomposition temperature of most OA was lower than that of pure OA

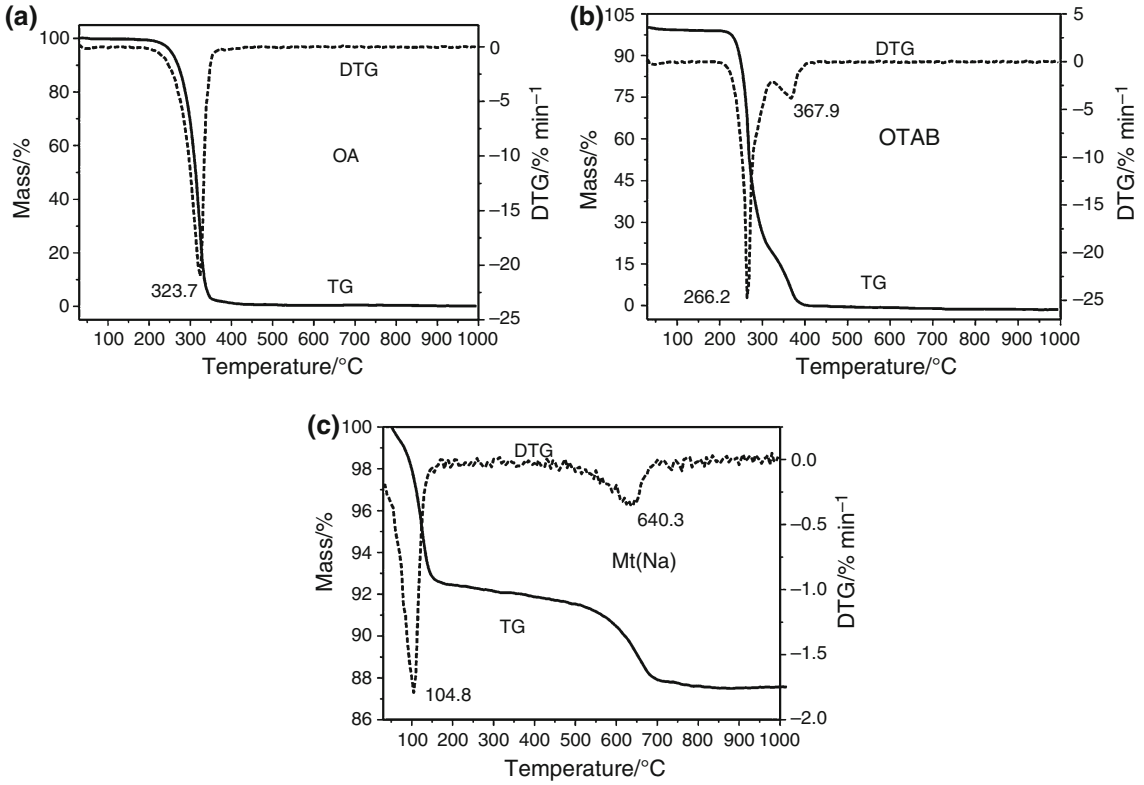

Fig. 3 TG and DTG curves for OA (**a**), OTAB (**b**) and Mt(Na) (**c**)

Table 2 Percentage of mass loss for OA, OTAB, Mt-OA complex and Mt-OTAB complexes at different temperature levels

Sample	Stage 1 mass loss/<200 °C		Stage 2 mass loss/200–500 °C		Stage 3 mass loss/>500 °C	
	°C	%	°C	%	°C	%
Mt(Na)	104.8	7.6	/	0.0	640.3	3.6
Pure OA	/	0.0	323.7	98.1	/	0.0
OA-Mt(Na)	99.7	6.9	275.2	19.9	/	/
Pure OTAB	/	0.0	266.2/367.9	100.0	/	0.0
OTAB-Mt(Na)	97.9	6.0	262.1	20.3	/	/
$OTAB_{inter}$-Mt(Na)	93.9	2.9	321.1/424.4	28.2	/	/

(323.7 °C). This result may indicate that Mt(Na) has a catalytic effect on the thermal decomposition of OA. The inherent solid acidity of clay minerals may enable Mt(Na) to act as an efficient solid acid catalyst in organic reactions [32–36]. The third phase of mass loss occurred at a temperature of higher than 500 °C, primarily due to a decrease in structural water levels. Hydroxyl disappearance only contributed slightly to the thermal behavior of both OTAB and OA. Thus, no further discussion on this topic is included in this manuscript.

A comparative study on OTAB and Mt(Na) was performed to examine the role of the interlayer space. As shown in Fig. 5a, OTAB-Mt(Na), the simply mixed sample, shows thermal degradation characteristics that are a combination of those of pure OTAB and Mt(Na). A release of adsorbed and interlayer water in Mt(Na) occurred at temperatures of below 200 °C. The mass loss level reached approximately 6.0% at this stage, with a DTG peak at 97.9 °C (Table 2). The majority of the OTAB in OTAB-Mt(Na) evolved rapidly within a temperature range of 300–450 °C, within which a sharp DTG peak resolved at 262.1 °C. The small DTG peaks may be attributed to a small amount of OTAB that was unaffected by Mt(Na) and that decomposed spontaneously. The dehydroxylation of Mt(Na) at a temperature of more than 500 °C is negligible relative to the significant mass loss that occurred as a result

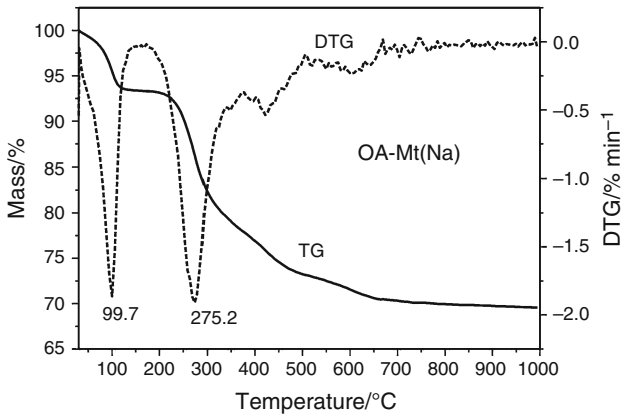

Fig. 4 TG and DTG curves for OA-Mt(Na)

of OTAB decomposition. The results show that the main decomposition temperature of OTAB-Mt(Na) (262.1 °C) is slightly lower than that of pure OTAB (266.2 °C), though this difference is minor, potentially indicating that no substantial change in the thermal decomposition behaviors of the simply mixed Mt(Na)-OTAB sample occurred. Compared to the OA-Mt(Na), the catalytic effect of Mt(Na) is not as great as that of OA in OA-Mt(Na). This result is due to the nature of OTAB, because the solid acid sites of Mt(Na) might induce different organic reactions, highly depending on the character of the functional group of organics. The carboxyl group is likely more sensitive to the acidic effect of Mt(Na) than that of amine group.

For the interlayer Mt(Na)–OTAB complex, the TG curve in the dehydration stage (below 200 °C) is much milder than that of Mt(Na) (Fig. 3c). The mass loss associated with the water content is only 2.9% for $OTAB_{inter}$-Mt(Na) compared to 7.6% for Mt(Na), denoting the replacement of hydrated sodium cations by OTAB. Thus, the DTG in this range of $OTAB_{inter}$-Mt(Na) decreases from 104.8 °C (for Mt(Na)) to 93.9 °C, as residual free water is easily removed at lower temperatures. The mass loss of the interlayer OTAB-Mt(Na) complex is approximately 28.2% within a temperature range of 200–500 °C. As described above, the initial content of OTAB in $OTAB_{inter}$-Mt(Na) is 30.3%. These data show that most organic matter is decomposed within the interlayer space. However, two peaks of organic matter degradation can be observed at 321.1 and 424.4 °C for the interlayer Mt(Na)-OTAB complex of the DTG curves shown in Fig. 5b. Similar results have been reported in previous reports [30, 37, 38]. For the DTG curves of organoclays, the first peak occurring at a low temperature is mainly attributed to the decomposition of organic molecules adsorbed on the inter-surface of clay minerals with Van der Waal force. Consequently, lower energy and temperature levels are needed for decomposition purposes, as these parts of organics are unstable. However, the second peak at a high temperature likely occurred as a result of the thermal cracking of ionic organics. This occurred because higher levels of energy are needed for these parts of organic ions to break down when positive amino groups combine with layers of montmorillonite via electrostatic forces [30, 37, 39, 40]. Therefore, the low-temperature peak in the DTG curve (the temperature of $OTAB_{inter}$-Mt(Na) is 321.1 °C) is attributable to molecular OTAB, and the second peak (the temperature of $OTAB_{inter}$-Mt(Na) is 424.4 °C) is attributable to ionic OTAB. Clearly, the thermal decomposition temperature of both the interlayer and OTAB is significantly higher than the corresponding temperature of pure OTAB (266.2 °C) and its simply mixed complex (262.1 °C). The results demonstrate that the interlayer structure of Mt(Na) can improve the thermal stability of intercalated OTAB, resulting in an increase in degradation temperatures.

The above analysis further implies that interacted OTAB can be preserved from the interlayer space structure of Mt(Na), and thermal behaviors are affected by combination features, as different decomposition temperatures were observed.

Possible effects of Mt(Na) on the thermal behavior of OA and OTAB

The above analysis shows that Mt(Na) leads to a lower decomposition temperature of OA but produces no

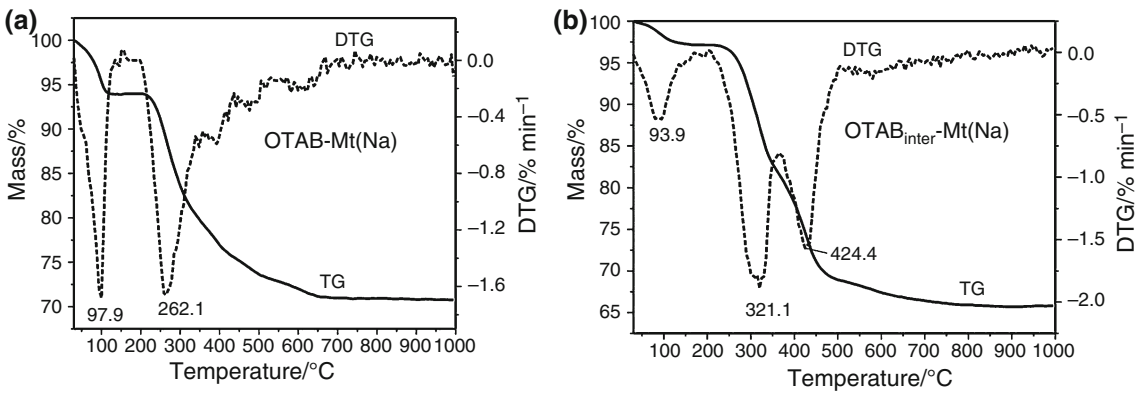

Fig. 5 TG and DTG curves for OTAB-Mt(Na) (**a**) and $OTAB_{inter}$-Mt(Na) (**b**)

substantial change for the simply mixed complex of OTAB. The decomposition temperature of OTAB-Mt(Na) is almost the same as that of pure OTAB. However, for the interlayer Mt(Na)-OTAB complex, the thermal decomposition temperature is significantly higher than the corresponding temperature of pure OTAB and its simply mixed complex. These results may indicate that Mt(Na) plays a dual role in the decomposition of OA. First, Mt(Na) may accelerate the thermal decomposition of OA, and the inherent solid acidity may be a key factor. As shown through previous studies, the Brønsted and Lewis acid sites coexist within the structure of Mt(Na) and offer a wide range of applications in organic reactions [33–35]. For instance, Brønsted acid sites can catalyze hydrogenation reactions, and Lewis acid sites can promote decarboxylation [1, 41, 42]. For simply mixed complexes, these Brønsted acid sites mainly derive from the external surface of Mt(Na), i.e., some surface-adsorbed H_3O^+. Although some Brønsted acid sites mainly arise from the interlayer space, these active sites may be limited in its capacity to promote thermal reactions, for they are away from the organic. Lewis acid sites arise from octahedral-coordinated Al^{3+} and/or Fe^{3+}ions exposed along the edges of Mt(Na) crystallites [36], which can capture an electron from OA in forming a radical intermediate. Through rearrangement, the radical intermediate then forms an alkyl radical and CO_2, as indicated by several studies [36, 41]. While Lewis acid along the edges of Mt(Na) crystallites may play a role, it is not the main mechanism that governs decarboxylation reactions. Reactions may also be affected by interlayer spaces and channels within clay minerals [5].

The interlayer structure of Mt(Na) may preserve OA and OTAB while increasing thermal stability levels. For instance, in the presence of Mt(Na), the decomposition temperature of OTAB is almost the same as that of pure OTAB. Instead, the thermal decomposition temperature of OTAB is further promoted in the interlayer space. OTAB, the special derivative of OA, is largely preserved. OA may be one of the components intercalated into the interlayer space of expanding clay minerals in sedimentary environments or clay-rich rocks. Thus, it can be inferred that the stability of OA may also be enhanced by Mt(Na).

Furthermore, in the presence of Mt(Na), the thermal decomposition behaviors of organic matter may also depend on its structures and composition. To the best of our knowledge, OA is a type of organic material that contains a carboxyl group. OTAB, a nitrogen-containing organic material, includes amino ions and is a derivative of OA. According to the above results, in the presence of Mt(Na), the thermal degradation temperature of OA was reduced. However, the thermal decomposition temperature almost remained the same for pure OTAB, whereas the thermal decomposition temperature increased when OTAB was located in the interlayer space of Mt(Na). This finding is not consistent with the result of previous works [36, 43, 44]. Recently, Liu et al. [36] studied the thermal degradation of clay–organic complexes with 12-aminolauric acid (ALA) and Mt. It is widely recognized that the decomposition temperature of ALA in mixed and interlayer complexes decreases to 402 and 342 °C, respectively. Pure ALA decomposed at 467 °C. This large difference may indicate that the thermal degradation of organic matter was closely related to the structure and composition of the organic matter used. In the presence of Mt(Na), thermal behaviors of fatty acid with a carboxyl group are easily catalyzed by Mt(Na), thereby lowering the decomposition temperature. By contrast, the thermal decomposition temperature of its derivative with an amino or amine structure in the presence of Mt(Na) is difficult to reduce, and thermal stability levels within the interlayer structure can be improved. It is universally acknowledged that in the presence of decarboxylase, amino acid may produce carbon dioxide and the corresponding amine through a decarboxylic reaction. Therefore, it can be inferred that organics with amino and amine structures are more stable than those with carboxyl groups in the presence of Mt(Na).

Conclusions

The thermal decomposition behavior of OA and OTAB in the presence of Mt(Na) was examined using TG/DTG methods. In the presence of Mt(Na), OA decomposed at 275.2 °C, thus decomposing sooner than pure OA (323.7 °C). However, the thermal decomposition behavior of OTAB is almost consistent with that of pure OTAB (266.2 °C), whereas for interlayer OTAB, the decomposition temperature increased to more than 300 °C. This demonstrates that Mt(Na) plays a dual role in the thermal degradation of OA. Mt(Na) accelerated the thermal decomposition of OA, and inherent solid acidity may play a major role. In addition, the interlayer structure of Mt(Na) enhanced the thermal stability of OA and OTAB. However, the thermal decomposition behaviors of organic matter may also depend on its structure and composition. When mixed with Mt(Na), OA and OTAB present very different thermal degradation behaviors. In the presence of Mt(Na), organics with amino and amine structures are more stable than those with carboxyl groups.

Acknowledgements This work was financially supported by the National Natural Science Foundation of China (Grant Nos. 41272059, 41472044, 41502031, and 41173069), Foundation of Guangdong (Grant No. 2015A030310363) and Guangzhou (Grant No. 201510010153)and CAS/SAFEA International Partnership Program for Creative Research Teams (Grant No. 20140491534). This is a contribution (no. IS-2318) from GIGCAS.

References

1. Jurg J, Eisma E. Petroleum hydrocarbons: generation from fatty acid. Science. 1964;144(3625):1451.
2. Shimoyama A, Johns WD. Catalytic conversion of fatty acids to petroleum-like paraffins and their maturation. Nature. 1971;232(33):140–4.
3. Galwey AK. The rate of hydrocarbon desorption from mineral surfaces and the contribution of heterogeneous catalytic-type processes to petroleum genesis. Geochim Cosmochim Acta. 1972;36(10):1115–30.
4. Johns WD. Clay mineral catalysis and petroleum generation. Annu Rev Earth Planet Sci. 1979;7:183–98.
5. Heller-Kallai L, Aizenshtat Z, Miloslavski I. The effect of various clay minerals on the thermal decomposition of stearic acid under 'bulk flow' conditions. Clay Miner. 1984;19(5):779–88.
6. Tannenbaum E, Kaplan IR. Role of minerals in the thermal alteration of organic matter—I: generation of gases and condensates under dry condition. Geochimicaet Cosmochimica Acta. 1985;49(12):2589–604.
7. Kennedy MJ, Pevear DR, Hill RJ. Mineral surface control of organic carbon in black shale. Science. 2002;295(5555):657–60.
8. Pan C, Jiang L, Liu J, Zhang S, Zhu G. The effects of calcite and montmorillonite on oil cracking in confined pyrolysis experiments. Org Geochem. 2010;41(7):611–26.
9. Keil RG, Tsamakis E, Fuh CB, Giddings JC, Hedges JI. Mineralogical and textural controls on the organic composition of coastal marine sediments: hydrodynamic separation using SPLITT-fractionation. Geochim Cosmochim Acta. 1994;58(2):879–93.
10. Mayer LM. Surface area control of organic carbon accumulation in continental shelf sediments. Geochim Cosmochim Acta. 1994;58(4):1271–84.
11. Schulten HR, Leinweber P. Characterization of humic and soil particles by analytical pyrolysis and computer modeling. J Anal Appl Pyrol. 1996;38(1):1–53.
12. Perez Rodriguez JL, Weiss A, Lagaly G. A natural clay organic complex from Andalusian black earth. Clays Clay Miner. 1977;25(3):243–51.
13. Lu XC, Hu WX, Fu Q. Study of combination pattern of soluble organic matters and clay minerals in the immature source rocks in Dongying depression, China. Scientia Geologica Sinica. 1999;34(1):69–72 **(in Chinese)**.
14. Cai J, Bao Y, Yang S, Wang X, Fan D, Xu J, Wang A. Research on preservation and enrichment mechanisms of organic matter in muddy sediment and mudstone. Sci China, Ser D Earth Sci. 2007;50(5):765–75.
15. Yuan P, Liu H, Liu D, Tan D, Yan W, He H. Role of the interlayer space of montmorillonite in hydrocarbon generation: an experimental study based on high temperature–pressure pyrolysis. Appl Clay Sci. 2013;75:82–91.
16. Theng BKG. The chemistry of clay–organic reactions. New York: Wiley; 1974.
17. Theng BKG, Churchman GJ, Newman RH. The occurrence of interlayer clay-organic complexes in two New Zealand solis. Soil Sci. 1986;142(5):262–6.
18. Lagaly G, Ogawa M, Dékány I. Clay minerals organic interactions. In: Bergaya F, Theng BKG, Lagaly G, editors. Handbook of clay science. Developments in clay science, vol. 1. Amsterdam: Elsevier; 2006. p. 309–58.
19. Faure P, Schlepp L, Burkle-Vitzthum V, Elie M. Low temperature air oxidation of n-alkanes in the presence of Na-smectite. Fuel. 2003;82(14):1751–62.
20. Li Z, Zhang ZL, Sun YH, Lao YX, Lin WZ, Wu WF. Catalytic decarboxylations of fatty acids in immature oil source rocks. Sci China Series D-Earth Sci. 2003;46(12):1250–60.
21. Zhang ZL, Ren YH, Yan ZL, Zhang TY. Kinetics on hydrocarbon generation from fatty acid ester in the presence of natural minerals at low temperature. Geochimica. 2005;34(3):263–8.
22. Xi Y, Ding Z, He H, Frost RL. Structure of organoclays—an X-ray diffraction and thermogravimetric analysis study. J Coll Interf Sci. 2004;277(1):116–20.
23. Li Z, Jiang WT, Hong H. An FTIR investigation of hexadecyltrimethylammonium intercalation into rectorite. Spectrochim Acta Part A Mol Biomol Spectrosc. 2008;71(4):1525–34.
24. He H, Ma Y, Zhu J, Yuan P, Qing Y. Organoclays prepared from montmorillonites with different cation exchange capacity and surfactant configuration. Appl Clay Sci. 2010;48(1):67–72.
25. Yuan P, Southon PD, Liu Z, Green ME, Hook JM, Antill SJ, Kepert CJ. Functionalization of halloysite clay nanotubes by grafting with γ-aminopropyltriethoxysilane. J Phys Chem C. 2008;112(40):15742–51.
26. Luo M, Guan P, Liu WH. The identification of several saturated fatty acids and their salts by means of infrared spectrometry. Spectrosc Spectral Anal. 2007;27(2):250–3 **(in Chinese)**.
27. He H, Frost RL, Zhu J. Infrared study of HDTMA + intercalated montmorillonite. Spectrochim Acta Part A Mol Biomol Spectrosc. 2004;60(12):2853–9.
28. Maher KD, Kirkwood KM, Gray MR, Bressler DC. Pyrolytic decarboxylation and cracking of stearic acid. Ind Eng Chem Res. 2008;47(15):5328–36.
29. Xie W, Gao Z, Pan WP, Hunter D, Singh A, Vaia R. Thermal degradation chemistry of alkyl quaternary ammonium montmorillonite. Chem Mater. 2001;13(9):2979–90.
30. He H, Ding Z, Zhu J, Yuan P, Xi Y, Yang D, Frost RL. Thermal characterization of surfactant-modified montmorillonites. Clays Clay Miner. 2005;53(3):287–93.
31. Hwu JM, Jiang GJ, Gao ZM, Xie W, Pan WP. The characterization of organic modified clay and clay-filled PMMA nanocomposite. J Appl Polym Sci. 2002;83(8):1702–10.
32. Bergaya F, Theng BKG, Lagaly G. Handbook of clay science, vol. 1. Amsterdam: Elsevier Science; 2006.
33. Reddy CR, Nagendrappa G, Jai Prakash BS. Surface acidity study of Mn^{+}-montmorillonite clay catalysts by FT-IR spectroscopy: correlation with esterification activity. Catal Commun. 2007;8(3):241–6.
34. Singh B, Patial J, Sharma P, Agarwal SG, Qazi GN, Maity S. Influence of acidity of montmorillonite and modified montmorillonite clay minerals for the conversion of longifolene to isolongifolene. J Mol Catal A Chem. 2007;266(1–2):215–20.
35. Liu H, Liu D, Yuan P, Tan D, Cai J, He H, Song Z. Studies on the solid acidity of heated and cation-exchanged montmorillonite using n-butylamine titration in non-aqueous system and diffuse reflectance Fourier transform infrared (DRIFT) spectroscopy. Phys Chem Miner. 2013;40(6):479–89.
36. Liu H, Yuan P, Qin Z, Liu D, Tan D, Zhu J, He H. Thermal degradation of organic matter in the interlayer clay–organic complex: a TG-FTIR study on a montmorillonite/12-aminolauric acid system. Appl Clay Sci. 2013;80:398–406.
37. Xi Y, Frost RL, He H. Modification of the surfaces of Wyoming montmorillonite by the cationic surfactants alkyl trimethyl, dialkyl dimethyl, and trialkyl methyl ammonium bromides. J Coll Interf Sci. 2007;305(1):150–8.
38. Vazquez A, López M, Kortaberria G, Martín L, Mondragon I. Modification of montmorillonite with cationic surfactants. Thermal and chemical analysis including CEC determination. Appl Clay Sci. 2008;41(1–2):24–36.
39. Zhu JX, He HP, Guo JG, Yang D, Xie XD. Arrangement models of alkylammonium cations in the interlayer of HDTMA + pillared montmorillonites. Chin Sci Bull. 2003;48(4):368–72.

40. Park Y, Ayoko GA, Kristof J, Horváth E, Frost RL. A thermoanalytical assessment of an organoclay. J Therm Anal Calorim. 2012;107(3):1137–42.
41. Alomon W, Johns W. Petroleum forming reactions: the mechanism and rate of clay catalyzed fatty acid decarboxiolation. In: Advance of organic geochemistry, 7th International Meeting; 1975. p. 157–71.
42. Geatches DL, Clark SJ, Greenwell HC. Role of clay minerals in oil-forming reactions. J Phys Chem A. 2010;114(10):3569–75.
43. Martins S, Fernandes JB, Mojumdar SC. Catalysed thermal decomposition of $KClO_3$ and carbon gasification. J Therm Anal Calorim. 2015;119(2):831–5.
44. Greathouse J, Johnson K, Greenwell H. Interaction of natural organic matter with layered minerals: recent developments in computational methods at the nanoscale. Minerals. 2014;4(2):519–40.